MitoNEET Protects HL-1 Cardiomyocytes from Oxidative Stress Mediated Apoptosis in an *In Vitro* Model of Hypoxia and Reoxygenation

Anika Habener[1,2], **Arpita Chowdhury**[1,3], **Frank Echtermeyer**[1], **Ralf Lichtinghagen**[4], **Gregor Theilmeier**[1,5◉], **Christine Herzog**[1◉]*

1 Department of Anesthesiology and Intensive Care Medicine, Hannover Medical School, Hannover, Germany, 2 Department of Pediatric Pneumology, Allergology and Neonatology, Hannover Medical School, Hannover, Germany, 3 Department of Cellular Biochemistry, University Medical Center Göttingen, Göttingen, Germany, 4 Institute for Clinical Chemistry, Hannover Medical School, Hannover, Germany, 5 Department of Health Services Sciences, Faculty of Medicine and Health Sciences, University of Oldenburg, Oldenburg, Germany

◉ These authors contributed equally to this work.
* herzog.christine@mh-hannover.de

Abstract

The iron-sulfur cluster containing protein mitoNEET is known to modulate the oxidative capacity of cardiac mitochondria but its function during myocardial reperfusion injury after transient ischemia is unknown. The purpose of this study was to analyze the impact of mito-NEET on oxidative stress induced cell death and its relation to the glutathione-redox system in cardiomyocytes in an *in vitro* model of hypoxia and reoxygenation (H/R). Our results show that siRNA knockdown (KD) of mitoNEET caused an 1.9-fold increase in H/R induced apoptosis compared to H/R control while overexpression of mitoNEET caused a 53% decrease in apoptosis. Necrosis was not affected. Apoptosis of both, mitoNEET-KD and control cells was diminished to comparable levels by using the antioxidants Tiron and gluta-thione compound glutathione reduced ethyl ester (GSH-MEE), indicating that mitoNEET-dependent apoptosis is mediated by oxidative stress. The interplay between mitoNEET and glutathione redox system was assessed by treating cardiomyocytes with 2-acetylamino-3-[4-(2-acetylamino-2-carboxyethylsulfanylthio-carbonylamino) phenylthiocarbamoylsulfanyl] propionic acid (2-AAPA), known to effectively inhibit glutathione reductase (GSR) and to decrease the GSH/GSSG ratio. Surprisingly, inhibition of GSR-activity to 20% by 2-AAPA decreased apoptosis of control and mitoNEET-KD cells to 23% and 25% respectively, while at the same time mitoNEET-protein was increased 4-fold. This effect on mitoNEET-protein was not accessible by mitoNEET-KD but was reversed by GSH-MEE. In conclusion we show that mitoNEET protects cardiomyocytes from oxidative stress-induced apoptosis during H/R. Inhibition of GSH-recycling, GSR-activity by 2-AAPA increased mitoNEET-protein, accompanied by reduced apoptosis. Addition of GSH reversed these effects suggesting that mitoNEET can in part compensate for imbalances in the antioxidative glutathione-

carbonylamino) phenylthiocarbamoylsulfanyl] propionic acid; DCF-DA, 2',7'-dichlorofluorescin diacetate; GAPDH, glyceraldehyde-3-phosphate dehydrogenase; GSH, glutathione; GSH/GSSG, reduced glutathione to oxidized glutathione; GSH-MEE, glutathione compound glutathione reduced ethyl ester; GSR, glutathione reductase; HL-1 cells, murine cardiomyocyte cell line; HPRT, hypoxanthine phosphoribosyltransferase; H/R, hypoxia and reoxygenation; KD, knockdown; LDH, lactate dehydrogenase; ROS, reactive oxygen species; scr-siRNA, non-specific small interfering RNA; siRNA, small interfering RNA.

system and therefore could serve as a potential therapeutic approach for the oxidatively stressed myocardium.

Highlights

- MitoNEET protects cardiomyocytes from oxidative stress induced apoptosis
- Chemical inhibition of glutathione reductase activity by 2-AAPA reduces apoptosis and increases mitoNEET protein
- Addition of reduced glutathione reverses the effects of 2-AAPA

Introduction

Oxidative stress is a critical factor for the enlargement of myocardial damage during reperfusion injury after transient myocardial ischemia [1–3] by inducing cardiomyocyte death through apoptosis and necrosis [4, 5]. One option to therapeutically counteract myocardial cell death is to sustain the antioxidative capacity of the myocardium.

MitoNEET is a ubiquitously expressed iron-sulfur (Fe-S) protein with putative antioxidative capacity and with the highest level of mRNA seen in the heart [6]. Initially mitoNEET was discovered as a binding partner of pioglitazone, an insulin-sensitizing drug used in type 2 diabetes. The protein is located in the outer mitochondrial membrane by a N-terminal anchor and its C-terminus is facing towards the cytoplasm [6]. According to its crystal structure mitoNEET is a homodimer with one [2Fe-2S] cluster in each monomer [7, 8]. Fe-S cluster containing proteins exhibit multiple functions depending on cluster ligands, their orientations and the local hydrogen-bonding arrangement [9]. In particular, they often take part in dynamic redox-sensitive activities; act as electron transport mediators; regulatory agents in gene expression and enzyme activity; act as a depot for sulfur as well as iron; and sensors for cellular oxygen [10–12]. In fact, in the last few years the role of mitoNEET as a redox-active protein has been described in several disease models like obesity [13], cancer [14] and inflammation-induced Parkinson`s disease [15]. However, its role in cardiovascular disease states that are associated with oxidative stress induced damage has not been characterized yet.

The glutathione (GSH) redox system is one of the main antioxidative defence systems in cardiomyocytes [4]. The relevance of glutathione-dependent processes was demonstrated by augmented ischemic tissue damage after GSH depletion [16] and transient reduction of glutathione content connected with diminished activity of the enzyme glutathione reductase (GSR) [17] that reconstitutes the antioxidative form of glutathione [18].

In this study we aim to analyze the role of mitoNEET as a putative antioxidative motif and its interaction with known antioxidative systems like the glutathione reductase system during myocardial oxidative stress. For this purpose we used an *in vitro* model of hypoxia and reoxygenation (H/R)-induced apoptosis in HL-1 cardiomyoblast-like cells [19–22]. We chose the model of H/R since chronic hypoxia alone does not cause apoptosis in cardiomyocytes in cell culture [23]. In the first step, we examined the influence of mitoNEET on oxidative stress mediated cell death. Secondly we analyzed the interplay between mitoNEET and the glutathione redox-system.

Materials and Methods

Cell culture

For all cell culture experiments the murine cardiomyocyte cell line HL-1 (a kind gift of Prof. W. C. Claycomb, Louisiana State University, New Orleans, LA, USA) was used. HL-1 cells are a derivative of AT-1 cardiac myocytes, derived from an atrial tumor isolated from transgenic mice, in which the expression of simian virus 40 large T antigen was controlled by the atrial natriuretic factor promotor [20, 24]. HL-1 cells were cultured as described previously [20, 25].

One day after plating HL-1 cells were transfected with 40 pmol small interfering RNA (siRNA) to mitoNEET (28929, Applied Biosystems, Darmstadt, Germany) or non-specific (scr)-siRNA (1027281, Qiagen, Hilden, Germany) using Lipofectamine RNAiMAX (Invitrogen, Karlsruhe, Germany) under serum-free conditions (Opti-MEM I Reduced Serum Medium, GlutaMAX, Gibco, Darmstadt, Germany) based on the manufacturer`s instructions. Respective siRNAs with alternative backbones delivered comparable results. 30 hours after transfection cells were washed and maintained in minimal medium (without serum and norepinephrine) over night. Cells were subjected to normoxia (5% CO_2, 95% room air, 37°C) or simulated hypoxia (0.8% O_2, 94.2% N_2, 5% CO_2, 37°C) in media that was buffered according to hypoxic or normoxic conditions to target a stable pH and pCO_2 as described elsewhere [26]. After 3 hours cells were washed carefully and maintained in minimal medium for 1 hour during reoxygenation (H/R). Where indicated, cells were treated with GSR-inhibitor 2-acetylamino-3-[4-(2-acetylamino-2-carboxyethylsulfanylthiocarbonylamino) phenylthiocarbamoylsulfanyl] propionic acid (2-AAPA, 10 µM, dissolved in DMSO), the antioxidants Tiron (10 mM, dissolved in water) and glutathione reduced ethyl ester (GSH-MEE, 2 mM, dissolved in water, all Sigma-Aldrich, Munich, Germany) 30–60 minutes before and during H/R.

Protein overexpression

Mouse mitoNEET cDNA (genbank accession number NM_134007) was PCR amplified from position 96 to 422 with primer 5′ –AC GCTAGC T GACT ATG GGC CTC AGC TCC AAC T–3′ and 5′ –AC GAATTC AGC TTA GGT TTC CTT TTT CTT GAT GA–3′ using mouse HL-1 cDNA and subcloned into the expression vector pcDNA3.1 (Invitrogen, Karlsruhe, Germany). One day after plating HL-1 cells were transfected with 1 µg pcDNA3.1 or mitoN-pcDNA3.1 using X-tremeGENE™ 9 Transfection Reagent (Sigma-Aldrich, Munich, Germany) based on the manufacturer`s instructions. 30 hours after transfection cells were maintained in minimal medium overnight and subjected to H/R as described before.

Real-time RT-PCR

Total RNA was extracted from HL-1 cells using TRItidy reagent (Applichem, Darmstadt, Germany) and measured photometrically at 260/280 nm. Reagents and primers were obtained from Eurogentec (Cologne, Germany). 500 ng of total RNA was applied for reverse transcription using Reverse Transcriptase Core kit according to the manufacturer`s protocol. cDNA was diluted 1:1 in DNase-, RNase- and protease-free water (Applichem, Darmstadt, Germany) and 0.5 µl template was used.

Sequences of primer-pairs were as follows: mouse mitoNEET forward, 5′ –CGCTAAAGA GAATCGCACCAAAGC–3′, and mitoNEET reverse, 5′ –GCCTCGCAACTGTCCATTAGGTTT–3′; mouse HPRT forward, 5′ –TGATCAGTCAACGGGGGACATA–3′, and HPRT reverse, 5′ –GCCTGTATCCAACACTTCGAGA–3′. For real-time RT-PCR MESA-GREEN qPCR MasterMix Plus for SYBR Assay was used based on the manufacturer`s procedure. Signals generated by integration of MESA-GREEN into the amplified DNA were detected in a real-time machine

(Rotogene 3000, Corbett Life Science, Hilden, Germany) and normalized to hypoxanthine phosphoribosyltransferase (HPRT) gene expression. Data are expressed as $2^{-\Delta\Delta CT}$.

Lactate dehydrogenase (LDH)

Cell culture supernatants were harvested after H/R and LDH concentrations were measured as U/L using the LDH IFCC kit (Modular P, Roche Diagnostics, Mannheim, Germany) by a routine clinical analyzer (Hitachi 917, Hitachi Ltd, Tokyo, Japan). Data are expressed as % of hypoxic control.

Generation of polyclonal mitoNEET antibodies

Rabbit polyclonal antibodies specific for mitoNEET were generated by 28-day protocol using a double peptide strategy (Eurogentec, Seraing, Belgium). Two separate peptide sequences (EP083398: H2N-VHAFDMEDLGDKA+C-CONH2 and EP083397: H2N-C+LAYKKFYAKE NRTKA-CONH2) corresponding to mouse mitoNEET-protein (UniProt ID: Q91WS0) were synthesized and boosted by keyhole limpet hemocyanin, a non-Freunds adjuvant. Two rabbits were immunized 4 times with both mitoNEET peptides. Polyclonal anti-sera of both hosts were affinity purified against the injected peptides respectively. Specificity of the polyclonal antibodies was verified by siRNA transfection and competition experiments by Western Blot as well as mitochondrial localization by immunofluorescence microscopy. Due to its higher specifity the polyclonal antibody against peptide EP083398 of rabbit SY1094 was chosen for further studies (see S1 Protocol and S1 Fig).

Western Blot analysis

HL-1 cells were harvested with RIPA lysis buffer (50 mM Tris-HCl pH 7.4, 150 mM NaCl, 1% Nonidet P-40, 0.1% SDS, 0.5% Sodiumdesoxycholate) supplemented with phosphatase and protease inhibitors (PhosStop and Complete Mini, Roche Applied Science, Mannheim, Germany) and protein concentration of the supernatants were determined by Pierce BCA Protein Assay Kit (Thermo Scientific, Karlsruhe, Germany). Protein lysates (0,6–10 µg) were separated on 4–20% Tris-glycine gels (PAGEr Precast Gels, Lonza, Cologne, Germany) under reducing conditions. Proteins were blotted on PVDF membranes (Milipore, Darmstadt, Germany) for 1 hour which were then blocked with 5% nonfat dry milk in Tris buffered saline supplemented with 0.05% Tween20 (TBST 0.05%), 4% BSA/TBST 0.05% or 4% IgG-free, protease-free BSA/TBST 0.1% for 1 hour at room temperature (RT). Membranes were incubated with the following primary antibodies over night at 4°C: mitoNEET (diluted 1:20000 in 4% BSA/TBST 0.05%); glutathione reductase (ABIN233969, Antibodies Online, Aachen, Germany, diluted 1:5000 in 5% nonfat dry milk/TBST 0.05%), cleaved caspase-3 (no. 9661, Cell Signaling, Frankfurt, Germany, diluted 1:2000 in 4% IgG-free, protease-free BSA/TBST 0.1%). Horseradish-peroxidase-coupled rabbit IgG was used as secondary antibody (R1364HRP, Acris, Herford, Germany or P0448, Dako, Hamburg, Germany, diluted 1:2000–1:20000 in BSA or nonfat dry milk/TBST). The blots were detected on a ChemiSmart 5100 station (Vilbert Lourmat, Eberhardzell, Germany) by using Amersham ECL Plus Western Blotting Detection System (GE Healthcare, Braunschweig, Germany). Density of bands were quantified using Bio1D software (Vilber Lourmat, Eberhardzell, Germany). To correct signals for equal protein loading, membranes were re-probed with anti-Glyceraldehyde-3-Phosphate Dehydrogenase (GAPDH) (no. 2118, diluted 1:2000), anti-β-tubulin (no. 2146, diluted 1:1000–1:5000) or anti-β-actin (no. 4967, diluted 1:5000, all Cell Signaling, Frankfurt, Germany). Data are expressed as % of H/R control.

Apoptosis-Assays

Apoptosis was assessed by dectection of cleaved caspase-3 in Western Blot (see Western Blot analysis) and by TdT-mediated dUTP-biotin nick end labeling (TUNEL) method using the MEBSTAIN Apoptosis Kit II according to the manufacturer's instructions (MBL,Woburn, MA, USA).

Measurement of intracellular Reactive Oxygen Species (ROS) in HL-1 cells

Oxidative radicals generated in HL-1 cells were measured by using 2',7'-dichlorofluorescin diacetate (DCF-DA; Sigma-Aldrich, Munich, Germany). DCF-DA is an cell permeable probe, which is de-esterified intracellularly and becomes fluorescent after oxidation. 7×10^4 HL-1 cells were pre-incubated with 5 μM DCFH-DA in hypoxia-medium (see cell culture) for 15 min at 37°C. The fluorescence intensitiy was measured before hypoxia, after 3h hypoxia and after 3h hypoxia and 60 min reoxygenation in 12 well plates using a microplate reader (Spectrafluor Plus; Tecan, Crailsheim, Germany).

Glutathione reductase enzyme activity

Glutathione reductase (GSR)-activity was measured by a colorimetric glutathione reductase assay (no. K71-61-200, BioVision, Mountain View, CA, USA) where GSR reduces GSSG to GSH, which reacts with 5, 5′-Dithiobis (2-nitrobenzoic acid) (DTNB) to generate TNB^{2-} (yellow color, λ max = 405 nm). Samples and standards were detected at 405 nm in a microplate reader (Sunrise, Tecan, Crailshaim, Germany). The activity was calculated, normalized to protein amount (mU/mg protein) and expressed as % of H/R control.

Statistical analysis

For all statistical analysis GraphPad Prism software Version 5.0d was used (GraphPad Inc, San Diego, CA, USA). Data are presented as mean ± standard error of mean. Whenever data showed non-Gaussian distributions or significantly different standard deviations, Kruskal-Wallis test was used followed by Mann-Whitney-U test. Otherwise ANOVA was chosen followed by t-test.

Results

MitoNEET plays a role for oxidative stress induced apoptosis in cardiac HL-1 cells

In HL-1 cells knockdown of mitoNEET (mitoNEET-KD) expression by siRNA reduced both mitoNEET-mRNA and -protein to 25% quantified by real-time RT-PCR and Western Blot, respectively (S2 Fig). We observed an increase of 1.9 fold in caspase-3 activity in the mitoNEET-KD cells after H/R compared to hypoxic control cells (Fig 1A, 1E and 1F). However, no effect was observed on necrosis measured by LDH release (Fig 1B). This demonstrated that mitoNEET-KD elevates apoptosis but not necrosis. In order to prove a direct cytoprotective effect of mitoNEET we overexpressed mitoNEET in HL-1 cells (Fig 1C) and observed a 53% reduction of active caspase-3 after H/R in mitoNEET overexpressing cells compared to hypoxic control cells (Fig 1D and S3 Fig). Addition of antioxidative superoxide scavenger Tiron (10 mM) decreased H/R-induced apoptosis of control cells to 60% (Fig 1E and 1F) as well as apoptosis of mitoNEET-KD cells to the same level indicating that mitoNEET-counteracted apoptosis was caused by superoxide radicals and was consequently related to reactive oxygen
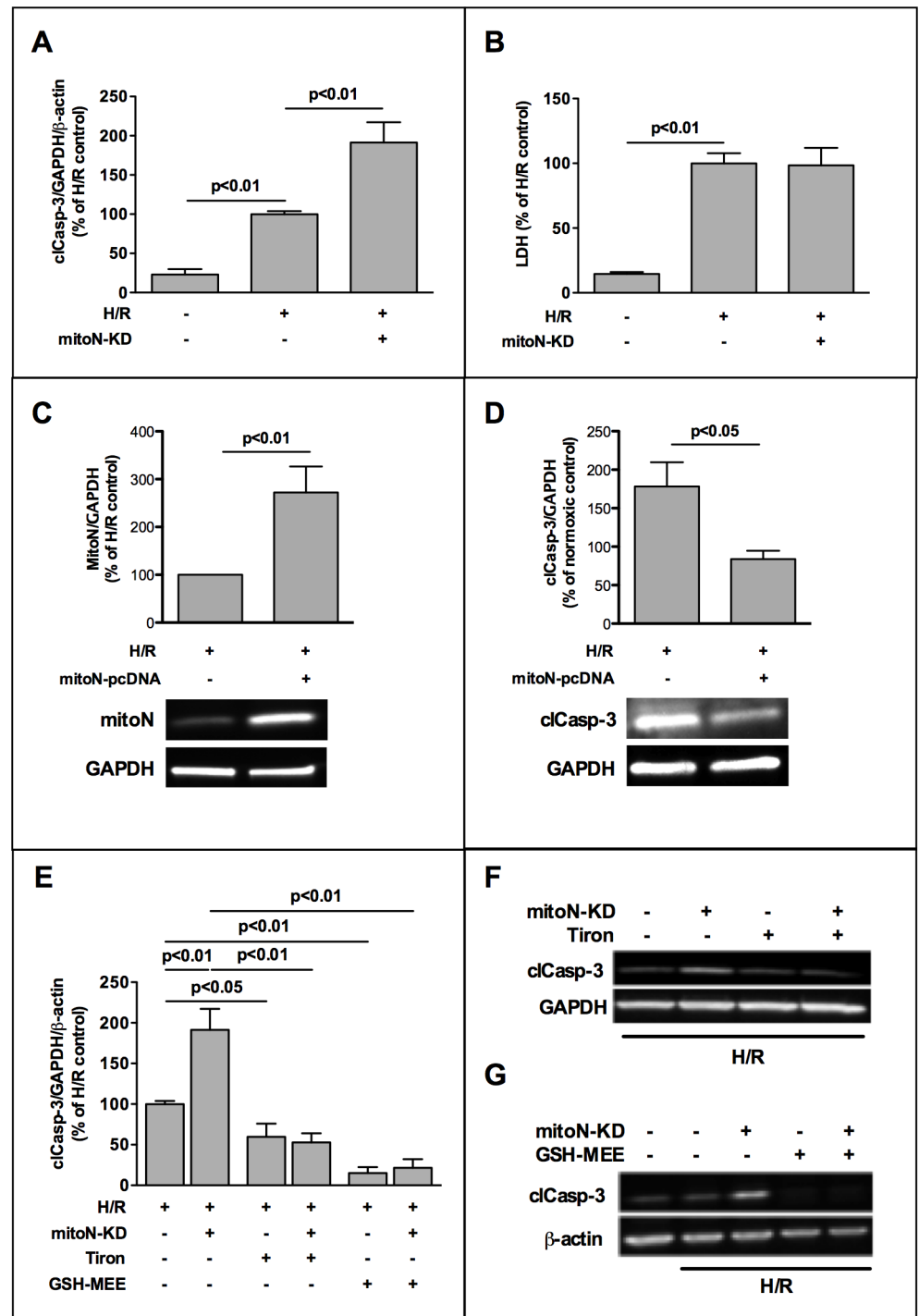
Fig 1. MitoNEET plays a role for oxidative stress induced apoptosis in cardiac HL-1 cells. HL-1 cells were transfected with silencing RNA (siRNA) directed against mitoNEET and non-specific-siRNA as control and subjected to 3h hypoxia followed by 1h of reoxygenation (H/R). (A) Densitometric analysis of Western Blots revealed aggravated activation of caspase-3 in mitoNEET-knockdown (mitoN-KD) cells after H/R compared to hypoxic controls (n = 11). (B) MitoNEET-KD showed no effect on lactate dehydrogenase (LDH) release after H/R measured in culture supernatants (n = 10). LDH was quantified as U/L by a routine clinical analyzer and is expressed as % of H/R control. (C,D) Overexpression of mitoNEET in HL-1 cells caused a significant decrease in apoptosis in mitoNEET overexpressing cells compared to H/R control cells. Expression of mitoNEET (n = 5) and cleaved caspase (n = 7) is shown in representative Western Blots and

was densitometrically measured as % of H/R control. (E-G) H/R-induced apoptosis in control- and mitoNEET-KD cells was reduced by two different antioxidants, superoxide scavenger Tiron (10 mM, n = 5) and esterified glutathione compound GSH-MEE (glutathione reduced ethyl ester, 2 mM, n = 6) as demonstrated by representative Western Blots (F-G). Data were analyzed densitometrically, normalized to housekeeping gene expression and are expressed as % of H/R control.

doi:10.1371/journal.pone.0156054.g001

species (ROS). To assess the role of glutathione redox system in our H/R model, we used glutathione reduced ethyl ester (GSH-MEE) (Fig 1E and 1G), an esterified glutathione compound that is readily transported into the cell and increases intracellularly the bioavailability of glutathione [27]. GSH-MEE reduced apoptosis of both, hypoxic control- and mitoNEET-KD cells to the level of normoxic cells.

MitoNEET has no impact on H/R induced intracellular ROS-production

To analyze whether ROS play a role in our *in vitro* H/R-model we used the fluorescence probe DCF-DA to measure intracellular ROS. Our data show that after 3h hypoxia intracellular ROS is 2.6 fold and after 3h/1h H/R hypoxia even 5.4 fold increased compared to normoxic control cells (Fig 2). Addition of antioxidative superoxide scavenger Tiron (10 mM) decreased H/R-induced ROS-production by 91% and GSH-MEE (2 mM) by 70%, respectively. However, mitoNEET-KD doesn't show any effect on the amount of intracellular ROS measured within this cell culture system.
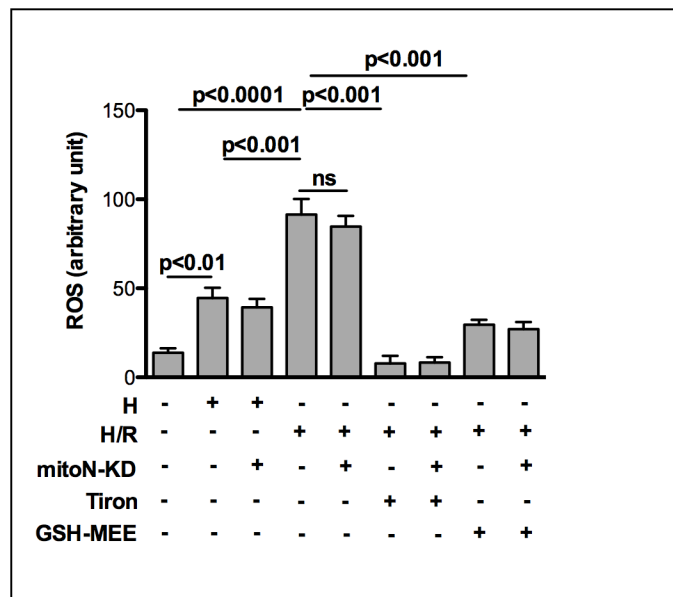
Fig 2. Intracellular ROS-production in HL-1 cells is not directly affected by mitoNEET. HL-1 cells were transfected with silencing RNA (siRNA) directed against mitoNEET and non-specific-siRNA as control and subjected to 3h hypoxia followed by 1h of reoxygenation (H/R). Using the fluorescent probe DCF-DA intracellular ROS-production was analyzed in a microplate reader. After 3h hypoxia intracellular ROS is 2.6 fold and after 60 min of reoxygenation even 5.4 fold increased compared to normoxic control cells (n = 12). Addition of antioxidative superoxide scavenger Tiron (10 mM; n = 6) and GSH-MEE (2 mM; n = 9) reduced the amount of ROS significantly. MitoNEET-KD doesn't show any effect on the amount of intracellular ROS measured within the different conditions.

doi:10.1371/journal.pone.0156054.g002

Chemical inhibition of glutathione reductase (GSR)-activity by 2-AAPA reduces oxidative stress induced apoptosis

Based on the literature we know that GSR-activity is decreased in rodent and human myocardial infarction and myocardial ischemia with reperfusion [28–30]. To analyze the role of GSR-activity in our H/R model we used 2-AAPA as an chemical inhibitor to effectively knockdown GSR-activity and to diminish the GSH/GSSG ratio causing an accumulation of GSSG [31–34].

Treatment of HL-1 cells with 10 µM 2-AAPA reduced GSR-activity to 20% (Fig 3A) without affecting GSR-protein expression (S4 Fig).

Inhibition of GSR-activity by 2-AAPA decreased apoptosis to 22% compared to H/R control (Fig 3B and 3C). To confirm this effect of 2-AAPA on H/R induced apoptotic cell death, we used TdT-mediated dUTP-biotin nick end labeling (TUNEL) method to visualize DNA fragmentation and observed a reduced amount of TUNEL-positive nuclei in 2-AAPA treated cardiomyocytes compared to H/R control cells (Fig 3D).

MitoNEET is increased by 2-AAPA

To elucidate the underlying mechanism that governs the surprising effect of 2-AAPA on apoptosis we analyzed the impact of 2-AAPA treatment on mitoNEET expression after H/R. While mitoNEET expression is not different at mRNA- and protein-level in normoxic- compared to H/R treated HL-1 cells (Fig 4A–4C), 2-AAPA results in a mild, but not significant, elevation of mitoNEET-mRNA (Fig 4A) and a robust 4-fold increase in mitoNEET-protein (Fig 4B and 4C).

2-AAPA decreases H/R-induced apoptosis and increases mitoNEET-protein despite of mitoNEET-knockdown

Our data show that knockdown of mitoNEET aggravates cardiac apoptosis during H/R and GSR-inhibition by 2-AAPA increases mitoNEET amount along with decreased apoptosis. Based on these findings we were interested in the effect of 2-AAPA on apoptosis in mitoNEET-KD cells. The combination of 2-AAPA with mitoNEET-KD reversed the proapoptotic effect of mitoNEET-KD and resulted in a significant decrease of cleaved caspase-3 to a similar level as observed in H/R cells treated with 2-AAPA only (Fig 5A). On mRNA level siRNA treatment effectively reduced mitoNEET-mRNA level in the presence of 2-AAPA in H/R treated KD-cells (Fig 5B). In mitoNEET-KD-cells treated with 2-AAPA mitoNEET-protein was significantly higher than in mitoNEET-KD-cells without 2-AAPA and comparable to increased mitoNEET-protein in H/R cells treated with 2-AAPA (Fig 5C).

Effect of 2-AAPA on mitoNEET can be reversed by GSH

To examine whether the effect of 2-AAPA on mitoNEET-protein was directly related to inhibition of GSR-activity and subsequently to GSH/GSSG ratio we added 2 mM GSH-MEE to H/R treated HL-1 cells which completely blocked the 2-AAPA induced mitoNEET increase (Fig 6) indicating that mitoNEET-protein is regulated by the redox state of the glutathione system. To address the question whether treatment of HL-1 cells with 2-AAPA and GSH-MEE shows an effect on the localization of mitoNEET within the cells we performed double immunofluorescence stainings using the mitochondrion-selective dye MitoTracker (100 nM) and rabbit anti-mitoNEET antibody (1:500). Using a 60x objective together with a 1.6x magnification changer we observed a mitochondrial colocalization of mitoNEET with MitoTracker in normoxic as well as in H/R-treated HL-1 cells, which was not affected by treatment of cells with 2-AAPA and GSH-MEE (S5 Fig).
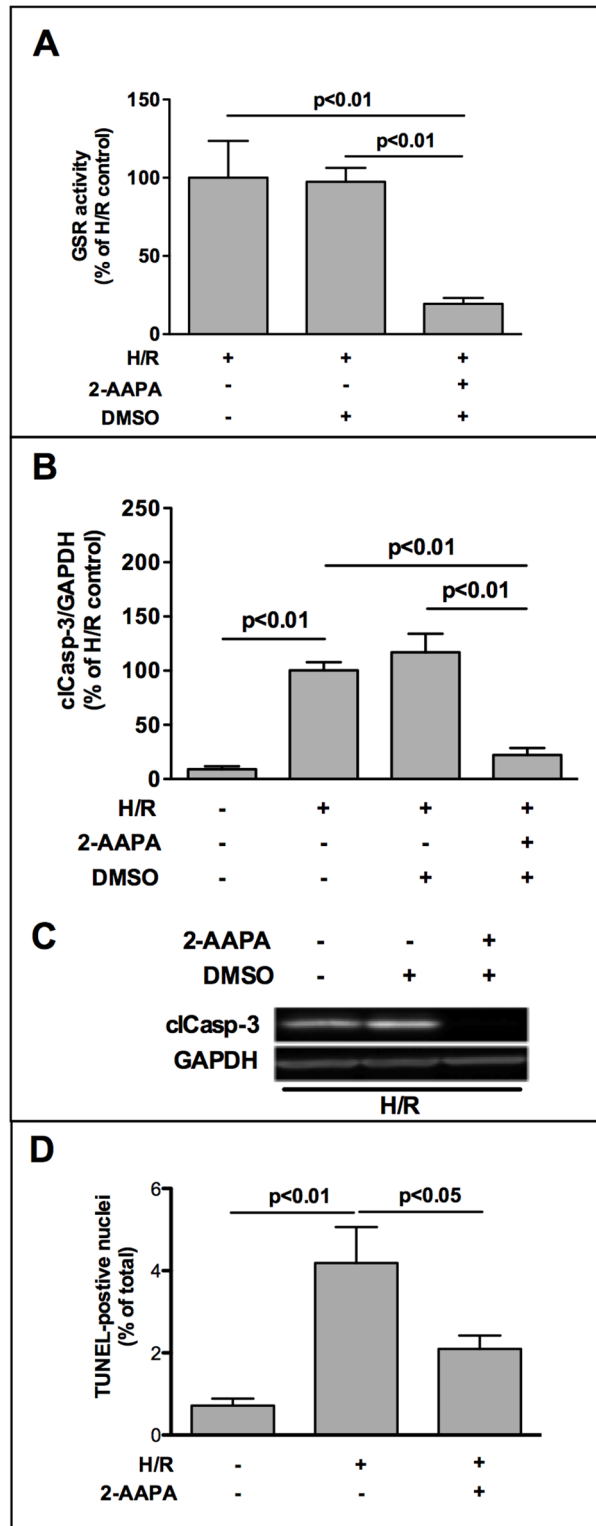
Fig 3. Chemical inhibition of glutathione reductase (GSR) reduces oxidative stress-induced apoptosis. (A) Chemical GSR-inhibitor 2-AAPA (10 µM) reduced GSR-activity to 20% (n = 5). GSR-activity was determined by a colorimetric glutathione reductase assay. Thereby GSR reduces GSSG to GSH that reacts with 5, 5′-Dithiobis (2-nitrobenzoic acid) (DTNB) to generate yellow TNB^{2-}, which was measured at 405 nm in a microplate reader. GSR-activity was calculated, normalized to protein amount (mU/mg protein)

and is expressed as % of H/R control. (B) Blockade of GSR-activity by 10 µM 2-AAPA decreased levels of activated caspase-3 in HL-1 cells after H/R (n = 5). (C) Representative Western Blot image is shown. Data were densitometrically analyzed and are expressed as % of H/R control. (D) TUNEL staining was utilized to determine apoptosis in HL-1 cells by the use of MEBSTAIN Apoptosis Kit II according to manufacturer`s protocol (MBL, Woburn, MA, USA). Data are presented as TUNEL-positive nuclei per total nuclei (n = 5).

Discussion

The salient findings of this study are that (i) mitoNEET is an antiapoptotic protein, which protects cardiomyoblasts (HL-1 cells) from oxidative stress induced apoptosis during H/R and (ii) that inhibition of GSR-activity by 2-AAPA increases the amount of mitoNEET-protein and decreases apoptosis, while addition of GSH abolishes 2-AAPA induced mitoNEET increase (Fig 7). These results suggest that mitoNEET may partly compensate for imbalances in the antioxidative glutathione-system during oxidative stress conditions.

Several studies investigated the impact of mitoNEET in disease models, which are associated with oxidative stress like obesity [13], cancer [14] and inflammation-induced Parkinson`s disease [15]. Recently the novel thiazolidinedione mitoNEET ligand-1 has been reported to show a protective effect on cardiac stem cell survival under oxidative stress conditions [35]. However, the role of mitoNEET during myocardial ischemia and reperfusion injury, which is also related to increased oxidative stress has not been characterized yet.

In cardiovascular diseases generation of ROS is a critical factor [36, 37]. Counteracting oxidative stress with different antioxidants diminished injury and improved recovery from ischemia and reperfusion injury in laboratory studies [4, 38] but most attempts to carry this strategy into the clinical arena have failed or demonstrated conflicting results [4].
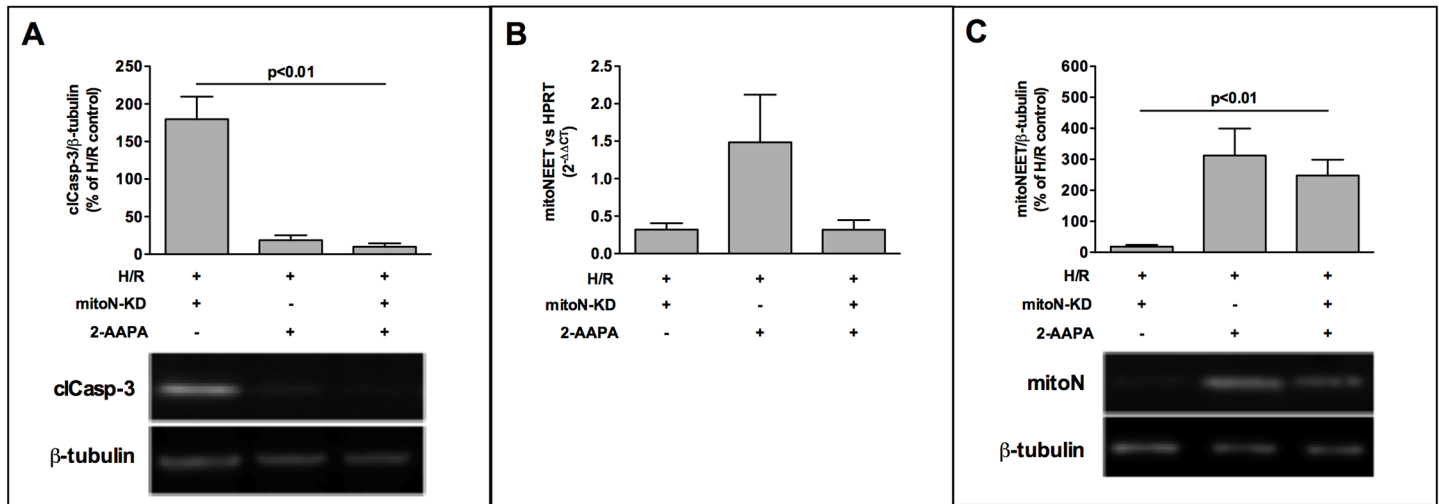
In order to better understand the functional role of mitoNEET in the context of ischemia and reperfusion we used the *in vitro* model of H/R induced apoptosis and show that reduced mitoNEET content increased apoptosis of cardiac HL-1 cells after H/R without showing an effect on necrosis supporting the critical role of mitoNEET as an antiapoptotic but not antinecrotic protein.

To analyze how oxidative stress dependent apoptosis is affected by mitoNEET we used the two different antioxidative compounds, Tiron and GSH-MEE [39, 40]. Protecting cells from superoxide by Tiron decreased apoptotic cell death and unmasked a mitoNEET-independent effect on apoptosis as well, suggesting that additional antioxidative systems are crucial in reducing ROS-related apoptosis in cardiomyocytes. Replenishing the intracellular pool of GSH
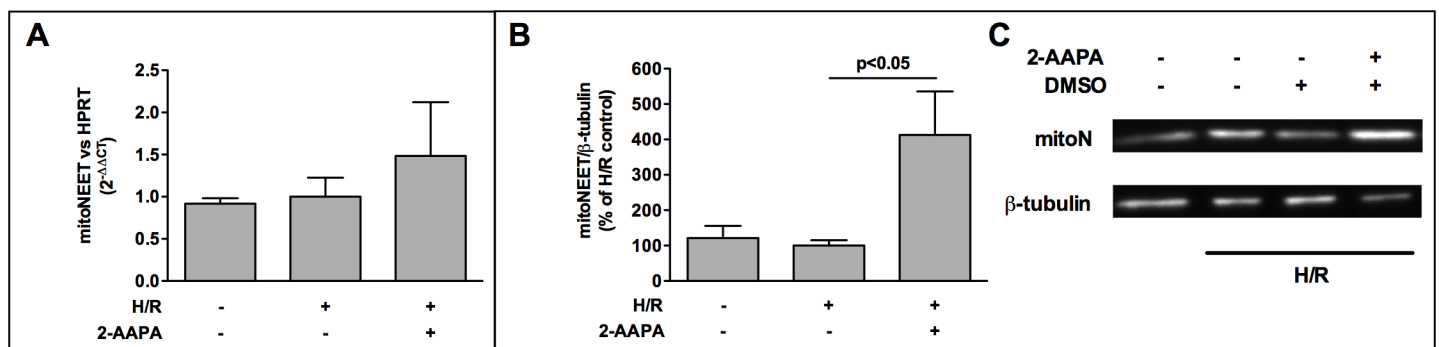

Fig 4. MitoNEET is increased by 2-AAPA. (A) Addition of GSR-inhibitor 2-AAPA (10 µM) led to a mild increase of mitoNEET-mRNA (n = 5) (B) while protein was increased 4-fold (n = 6) after H/R. (C) Representative Western Blots is presented. Data are expressed as % of H/R control. Real-time RT-PCR signals were normalized to hypoxanthine phosphoribosyl-transferase (HPRT) gene expression and data are expressed as $2^{-\Delta\Delta CT}$.
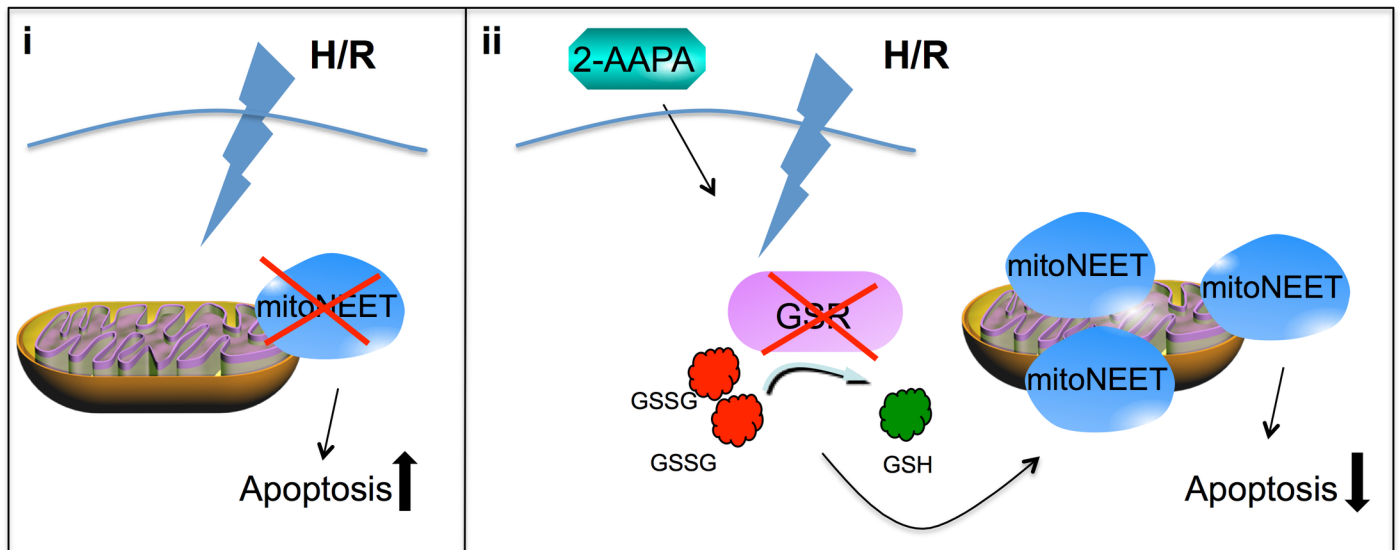
Fig 5. 2-AAPA decreases H/R induced apoptosis in mitoNEET-KD cells and increases mitoNEET-protein despite KD. (A) Western Blot analysis of activated caspase-3 revealed reduced apoptosis in 2-AAPA treated mitoNEET-KD cells to the same level seen in 2-AAPA treated HL-1 cells after H/R (n = 6). (B) siRNA transfection decreased mitoNEET-mRNA efficiently in the presence and absence of chemical GSR-inhibitor 2-AAPA (10 μM, n = 5) determined by real-time RT-PCR. (C) MitoNEET-protein of mitoNEET-KD-cells was significantly higher after addition of 2-AAPA compared to mitoNEET-KD-cells without 2-AAPA treatment (n = 5) measured after H/R. Representative Western Blots are shown (A, C) and data are expressed as % of H/R control. Real-time RT-PCR data are expressed as $2^{-\Delta\Delta CT}$.

doi:10.1371/journal.pone.0156054.g005
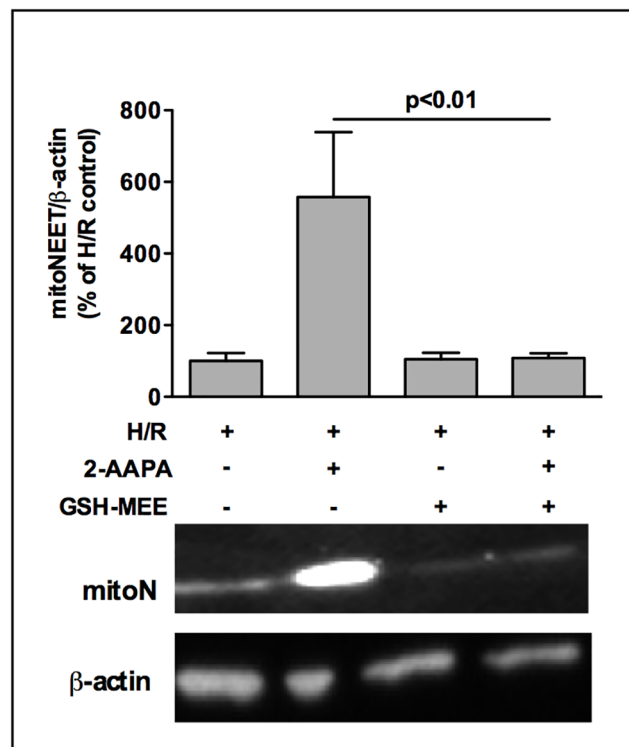
Fig 6. 2-AAPA effect on mitoNEET is abolished by addition of glutathione compound GSH-MEE. MitoNEET-protein amount of HL-1 cells was clearly increased after addition of GSR-inhibitor 2-AAPA (10 μM) determined after H/R by Western Blot. This effect was completely reversed by additon of glutathione compound GSH-MEE (2 mM, n = 4–5) as demonstrated by a representative Western Blot. Data are expressed as % of H/R control.

doi:10.1371/journal.pone.0156054.g006

Fig 7. Schematic view. (i) MitoNEET-knockdown increases oxidative stress induced apoptosis. (ii) 2-AAPA inhibits GSR activity and diminishes the GSH/GSSG ratio resulting in decreasesd H/R induced apoptosis and an increase in mitoNEET-protein.

by GSH-MEE, thereby protecting cells from ROS such as hydrogen peroxide and peroxynitrite [41], minimized apoptosis to the normoxic control level. These data indicate that mitoNEET constitutes a relevant part of the antioxidative capacity of the cardiomyocyte. Indeed, in mouse models of obesity, overexpression of mitoNEET in adipocytes and hepatocytes showed decreased ROS-induced damage, whereas a systemically induced knockdown of mitoNEET expression caused the opposite effect, [13] confirming the importance of mitoNEET in several disease states associated with oxidative stress. To assess the impact of mitoNEET on ROS homeostasis we measured intracellular ROS in our H/R-model. Recent studies showed that in embryonic fibroblasts lacking the 2Fe-2S-cluster containing NEET protein Miner1, also known as NAF-1, ROS-production was increased [42]. To our surprise, we couldn't detect a mito-NEET dependent effect on intracellular ROS production in our H/R-model. We do not know whether these differences between mitoNEET and NAF-1 are related to differences in the individual protein function or to differences in the *in vitro* cell culture models. Nevertheless, our data indicate that the presence of mitoNEET is important for mediating ROS-dependent apoptosis but it is not regulating ROS itself. It is well possible that mitoNEET interacts with other anti-apoptotic proteins or regulates the activity of anti-apoptotic enzymes. In this context it is of interest that NAF-1 was found to directly interact with Bcl-2 and Beclin 1 and therefore was proposed to regulate autophagy and apoptosis [43].

As a result of oxidative stress, reduced glutathione (GSH) is converted into its oxidized and antioxidative inactive form glutathione disulfide (GSSG). Reduced glutathione is reconstituted by GSR [18]. Several studies document decreased GSR-activity in animal models of myocardial infarction [30], ischemia and reperfusion [28] and in human patients with infarcted and reperfused hearts [29] which directed us to examine the interaction of GSR as a key enzyme of the glutathione redox system with mitoNEET-fostered anti-apoptotic effects. In our model of H/R GSR-activity was reduced (data not shown) suggesting that HL-1 cells constituted a good model for the *in vivo* situation. In order to investigate the influence of GSR-enzyme activity on H/R-dependent apoptosis we used 2-AAPA as a potent pharmacological inhibitior of the enzyme [31, 32, 34]. Reduction of GSR-activity to 20% by 2-AAPA surprisingly caused an

antiapoptotic effect suggesting that in case of an extreme imbalance of the glutathione redox-system a compensatory mechanism is induced. The individual regulation of the antioxidant capacity of different antioxidative enzymes and their mutual interactions are not fully understood. It is however conceivable that one antioxidant may compensate for another to maintain the cellular redox potential [44]. Interestingly, inhibition of GSR-activity by 2-AAPA increased mitoNEET-protein dramatically, and consequently apoptosis was significantly reduced. This increase of mitoNEET-protein is most likely due to regulatory processes on the protein level since we couldn't detect any major changes in mRNA expression of mitoNEET neither induced by H/R nor by 2-AAPA. To test, whether elevated mitoNEET-protein levels are directly caused by inhibition of GSH-restoring GSR-activity, we replenished intracellular GSH pool by addition of GSH-MEE, thereby avoiding 2-AAPA induced GSR-blockade. MitoNEET increase was completely abrogated by addition of GSH-MEE indicating that changes in glutathione availability can reverse the effect on mitoNEET-protein. In the same context a recent report by Laundry et. al. (2015) [45] showed that mitoNEET can be directly reduced by GSR in an NADPH-dependent reaction and further proposed a model for GSR-dependent redox transition of mitoNEET in response to oxidative stress. Our data support this model and add the finding that mitoNEET content is regulated by the redox state of the glutathione system suggesting a compensatory mechanism to protect cells from oxidative stress.

Nevertheless, the underlying mechanism by which decreased GSH-recycling GSR-activity increases mitoNEET content is unknown so far. 2-AAPA is a novel membrane-permeable compound that inhibits GSR-activity effectively by irreversible thiocarbamylation of GSR's active site thiols [31]. The inhibitor does not impair the antioxidative enzymes catalase and superoxide dismutase, the enzymes responsible for GSH biosynthesis γ-glutamylcysteine synthetase and glutathione synthase and only marginally influences glutathione peroxidase and glutathione S-transferase [31, 34]. In agreement, we and others show no influence on GSR-protein and -mRNA expression [34] by 2-AAPA, respectively. Since GSR catalyzes the reduction of GSSG to GSH [44], inhibition of GSR leads to GSSG accumulation and increases intracellular thiol oxidative stress [31]. However, Zhao et al. detected no changes in ROS formation during GSR inhibition by 2-AAPA [34]. During irradiation with generation of free radicals [46], 2-AAPA-mediated inhibition of GSR aggravated thiol oxidative stress and enhanced sensitivity of cancer cells to radiation [33]. Recently, it was shown that 2-AAPA is also able to inhibit GSR-related enzyme glutaredoxin-1 [47] and thioredoxin reductase [32] suggesting that in addition to GSR blockade a possible reduction of glutaredoxin-1- and thioredoxin-activity could additionally enlarge oxidative stress during H/R.

Our study is limited by the fact that a cardiomyocyte cell line was used. Therefore we cannot conclude that our results will also be valid in an *in vivo* model. Furthermore mitoNEET-knockdown was incomplete. Since there is no bioassay for mitoNEET available we were unable to directly measure mitoNEET antioxidative activity. Regulation of enzyme activity is therefore also an aspect that could be responsible for the observation presented here. Our attempt to visualize changes in the subcellular distribution of mitoNEET were limited by the resolution of our fluorescence imaging system in combination with H/R induced morphological alterations. To make a clear statement whether mitoNEET might move intracellularly after H/R and/or treatment with 2-AAPA using electron microscopy would be more appropiate.

In conclusion we show that mitoNEET protects intact cardiac cells from oxidative stress induced apoptosis during hypoxia and reoxygenation. Additionally our study demonstrates a previously unrecognized effect of the GSR inhibitor 2-AAPA, which increases mitoNEET-protein thereby setting off the prooxidative effects of GSR-inhibition. However, further studies are needed to clarify the mechanism by which mitoNEET is elevated as well as the resulting impact on cell viability *in vivo*.

Supporting Information

S1 Data. Original data sets.
(XLSX)

S1 Fig. Evaluation of polyclonal anti-mitoNEET antibody directed against peptide EP083398 in rabbit SY1094. (A) Knockdown (KD) of mitoNEET by small interfering RNA (siNRA) transfection diminished mitoNEET-protein detection in HL-1 cells as demonstrated by a representative Western Blot. (B) Incubation of murine fEnd.5 protein with mitoNEET-peptide EP083398 (ratio 1:5) showed reduced detection of mitoNEET-protein by Western Blot. (C) fEnd.5 cells were stained with mitochondrion-selective dye MitoTracker (100 nM) and incubated with rabbit anti-mitoNEET antibody (1:500) and fluorescein isothiocyanate-conjugated rabbit IgG (1:50) as secondary antibody. Nuclei were tagged with 1 µg/µl DAPI. Cell stainings were visualized by an inverted microscope (Olympus IX81) using a 60x objective together with a 1.6x magnification changer and photographed by a fluorescence camera (Retiga EXi). Characteristic fluorescent stainings of nuclei (blue), mitoNEET (green), MitoTracker (red) and colocalization of mitoNEET with MitoTracker in an Overlay (orange/ yellow) are shown.
(TIFF)

S2 Fig. MitoNEET expression of HL-1 cells after siRNA mediated mitoNEET-KD. (A-B) MitoNEET-mRNA (n = 12) and -protein (n = 14) amounts were reduced to 25% after mito-NEET-KD and hypoxia and reoxygenation (H/R) measured by real-time RT-PCR and Western Blot, respectively. A representative Western Blot is shown. Data were analyzed densitometrically, normalized to housekeeping gene expression and expressed as % of H/R control. Real-time RT-PCR signals were normalized to hypoxanthine phospho-ribosyltransferase (HPRT) gene expression and data are expressed as $2^{-\Delta\Delta CT}$.
(TIFF)

S3 Fig. Overexpression of mitoNEET reduces H/R induced apoptotic cell death. Control- and mitoNEET overexpressing-HL-1 cells were exposed to H/R. Apoptosis was detected and measured using the Cell-APOPercentage apoptosis assay (Biocolor, Tebu-bio, Offenbach, Germany) which uses a dye that is selectively imported by cells that are undergoing apoptosis. Shown are pictures of the labeled cells and the quantificiation of intracellular dye using a colorimetric assay (n = 5). Absorbance at 550 nm is measured in relative units.
(TIFF)

S4 Fig. GSR expression in HL-1 cells after inhibition with 2-AAPA. GSR-protein was not affected by application of chemical GSR-inhibitor 2-AAPA (10 µM, n = 4–5). DMSO as solvent showed no influence on GSR-protein. Representative Western Blot is shown and data are expressed as % of H/R control.
(TIFF)

S5 Fig. Localization of mitoNEET after treatment with 2-AAPA and GSH-MEE. HL-1 cells were treated with normoxia, H/R, H/R + 2-AAPA (10 µM) and H/R + 2-AAPA (10 µM) + GSH-MEE (2 µM). After treatment cells were stained with mitochondrion-selective dye MitoTracker (100 nM) and incubated with rabbit anti-mitoNEET antibody (1:500) and fluorescein isothiocyanate-conjugated rabbit IgG (1:50) as secondary antibody. Nuclei were tagged with 1 µg/µl DAPI. Cell stainings were visualized by an inverted microscope (Olympus IX81) using a 60x objective together with a 1.6x magnification changer and photographed by a fluorescence camera (Retiga EXi). Characteristic fluorescent stainings of nuclei (blue), mitoNEET (green), MitoTracker (red) and colocalization of mitoNEET with MitoTracker in an Overlay

(orange/ yellow) are shown.
(TIFF)

S1 Protocol. Evaluation of polyclonal anti-mitoNEET antibody generated against peptide EP083398 in rabbit SY1094. Peptide competition
Lyophilized peptide EP083398 corresponding to mouse mitoNEET-protein (UniProt ID: Q91WS0) was dissolved in 10% DMSO and combined with affinity purified polyclonal antibody (generated against peptide EP083398) in a 5-fold excess. Antigen-antibody solution was mixed by agitation (500 rpm) for 2 hours at room temperature. After centrifugation supernatant was diluted in 5% nonfat dry milk in Tris buffered saline supplemented with 0.05% Tween20 and used for incubation of protein lysates of fEnd.5 cells, a polyomavirus middle T antigen transformed murine endothelial cell line. Lysates were separated by SDS-PAGE and blotted on PVDF membranes. Protein was detected as described in Materials and Methods.
Mitochondrial localization
Immortalized mouse fEnd.5 cells [1,2] were plated on glass cover slips and cultured in Dulbecco`s modified Eagle`s medium supplemented with 10% fetal bovine serum, 1% L-glutamine and 1% penicillin/streptomycin until confluence. Cells were washed with PBS and incubated with 100 nM MitoTracker Orange CMTMRos (Invitrogen, Darmstadt, Germany) for 30 minutes at 37°C and prepared for indirect immunofluorescence staining as described previously [3] with some modifications. After fixation and quenching, cells were permeabilized with 0.5% saponin (Applichem, Darmstadt, Germany) in PBS for 10 minutes and washed twice with 0.1% saponin. Unspecific binding was blocked (5% normal goat serum, 0.1% saponin, 1% BSA in PBS) for 30 minutes and cells were washed three times with 1% BSA in PBS before incubation with anti-mitoNEET antibody (diluted 1:500 in 1% BSA in PBS) over night at 4°C in a wet chamber. Cells were washed 3 times with 0.1% saponin, 1% BSA in PBS. A fluorescein isothiocyanate-conjugated donkey anti-rabbit IgG antibody (Jackson ImmunoResearch, Suffolk, UK) was used as secondary antibody (diluted 1:50 in 0.1% saponin, 1% BSA in PBS) and DNA was colored blue with 1 µg/ml DAPI. Fluorescent stainings were visualised by an inverted microscope (Olympus IX81, Olympus, Muenster, Germany) using a 60x objective and a 1.6x magnification changer. Photos were taken by fluorescence camera Retiga EXi (QImaging, Buckinghamshire, United Kingdom).
Protocol apoptosis. (ii) 2-AAPA inhibits GSR activity and diminishes the GSH/GSSG ratio resulting in decreasesd H/R induced apoptosis and an increase in mitoNEET-protein.
(DOCX)

Acknowledgments

Author Contributions

Conceived and designed the experiments: AH GT CH. Performed the experiments: AH AC FE CH RL. Analyzed the data: AH FE GT CH. Wrote the paper: AH FE GT CH.

References

1. Ambrosio G, Zweier JL, Duilio C, Kuppusamy P, Santoro G, Elia PP, et al. Evidence that mitochondrial respiration is a source of potentially toxic oxygen free radicals in intact rabbit hearts subjected to ischemia and reflow. J Biol Chem. 1993; 268(25):18532–41. Epub 1993/09/05. PMID: 8395507.

2. Andreadou I, Iliodromitis EK, Farmakis D, Kremastinos DT. To prevent, protect and save the ischemic heart: antioxidants revisited. Expert Opin Ther Targets. 2009; 13(8):945–56. Epub 2009/06/19. doi: 10.1517/14728220903039698 PMID: 19534573.

3. Park JW, Chun YS, Kim YH, Kim CH, Kim MS. Ischemic preconditioning reduces Op6 generation and prevents respiratory impairment in the mitochondria of post-ischemic reperfused heart of rat. Life Sci. 1997; 60(24):2207–19. Epub 1997/01/01. S0024320597002361 [pii]. PMID: 9188764.

4. Kevin LG, Novalija E, Stowe DF. Reactive oxygen species as mediators of cardiac injury and protection: the relevance to anesthesia practice. Anesth Analg. 2005; 101(5):1275–87. Epub 2005/10/26. 101/5/1275 [pii] doi: 10.1213/01.ANE.0000180999.81013.D0 PMID: 16243980.

5. Tavazzi B, Di Pierro D, Bartolini M, Marino M, Distefano S, Galvano M, et al. Lipid peroxidation, tissue necrosis, and metabolic and mechanical recovery of isolated reperfused rat heart as a function of increasing ischemia. Free Radic Res. 1998; 28(1):25–37. Epub 1998/04/29. PMID: 9554830.

6. Wiley SE, Murphy AN, Ross SA, van der Geer P, Dixon JE. MitoNEET is an iron-containing outer mitochondrial membrane protein that regulates oxidative capacity. Proc Natl Acad Sci U S A. 2007; 104 (13):5318–23. Epub 2007/03/23. 0701078104 [pii] doi: 10.1073/pnas.0701078104 PMID: 17376863; PubMed Central PMCID: PMC1838440.

7. Lin J, Zhou T, Ye K, Wang J. Crystal structure of human mitoNEET reveals distinct groups of iron sulfur proteins. Proc Natl Acad Sci U S A. 2007; 104(37):14640–5. Epub 2007/09/04. 0702426104 [pii] doi: 10.1073/pnas.0702426104 PMID: 17766439; PubMed Central PMCID: PMC1976232.

8. Paddock ML, Wiley SE, Axelrod HL, Cohen AE, Roy M, Abresch EC, et al. MitoNEET is a uniquely folded 2Fe 2S outer mitochondrial membrane protein stabilized by pioglitazone. Proc Natl Acad Sci U S A. 2007; 104(36):14342–7. Epub 2007/09/04. 0707189104 [pii] doi: 10.1073/pnas.0707189104 PMID: 17766440; PubMed Central PMCID: PMC1963346.

9. Dicus MM, Conlan A, Nechushtai R, Jennings PA, Paddock ML, Britt RD, et al. Binding of histidine in the (Cys)3(His)1-coordinated [2Fe-2S] cluster of human mitoNEET. J Am Chem Soc. 2010; 132 (6):2037–49. Epub 2010/01/27. doi: 10.1021/ja909359g PMID: 20099820; PubMed Central PMCID: PMC2820139.

10. Beinert H, Holm RH, Munck E. Iron-sulfur clusters: nature's modular, multipurpose structures. Science. 1997; 277(5326):653–9. Epub 1997/08/01. PMID: 9235882.

11. Johnson DC, Dean DR, Smith AD, Johnson MK. Structure, function, and formation of biological iron-sulfur clusters. Annu Rev Biochem. 2005; 74:247–81. Epub 2005/06/15. doi: 10.1146/annurev.biochem.74.082803.133518 PMID: 15952888.

12. Sheftel A, Stehling O, Lill R. Iron-sulfur proteins in health and disease. Trends Endocrinol Metab. 2010; 21(5):302–14. Epub 2010/01/12. S1043-2760(09)00217-3 [pii] doi: 10.1016/j.tem.2009.12.006 PMID: 20060739.

13. Kusminski CM, Holland WL, Sun K, Park J, Spurgin SB, Lin Y, et al. MitoNEET-driven alterations in adipocyte mitochondrial activity reveal a crucial adaptive process that preserves insulin sensitivity in obesity. Nat Med. 2012; 18(10):1539–49. Epub 2012/09/11. doi: 10.1038/nm.2899 PMID: 22961109; PubMed Central PMCID: PMC3745511.

14. Sohn YS, Tamir S, Song L, Michaeli D, Matouk I, Conlan AR, et al. NAF-1 and mitoNEET are central to human breast cancer proliferation by maintaining mitochondrial homeostasis and promoting tumor growth. Proc Natl Acad Sci U S A. 2013; 110(36):14676–81. Epub 2013/08/21. doi: 10.1073/pnas.1313198110 PMID: 23959881; PubMed Central PMCID: PMC3767537.

15. Hunter RL, Choi DY, Ross SA, Bing G. Protective properties afforded by pioglitazone against intrastriatal LPS in Sprague-Dawley rats. Neurosci Lett. 2008; 432(3):198–201. Epub 2008/01/22. S0304-3940 (07)01282-7 [pii] doi: 10.1016/j.neulet.2007.12.019 PMID: 18207323; PubMed Central PMCID: PMC2699576.

16. Mizui T, Kinouchi H, Chan PH. Depletion of brain glutathione by buthionine sulfoximine enhances cerebral ischemic injury in rats. Am J Physiol. 1992; 262(2 Pt 2):H313–7. Epub 1992/02/01. PMID: 1539690.

17. Lievre V, Becuwe P, Bianchi A, Bossenmeyer-Pourie C, Koziel V, Franck P, et al. Intracellular generation of free radicals and modifications of detoxifying enzymes in cultured neurons from the developing rat forebrain in response to transient hypoxia. Neuroscience. 2001; 105(2):287–97. Epub 2001/10/24. PMID: 11672596.

18. Grant CM, Collinson LP, Roe JH, Dawes IW. Yeast glutathione reductase is required for protection against oxidative stress and is a target gene for yAP-1 transcriptional regulation. Mol Microbiol. 1996; 21(1):171–9. Epub 1996/07/01. PMID: 8843443.

19. Carlson DL, Lightfoot E Jr., Bryant DD, Haudek SB, Maass D, Horton J, et al. Burn plasma mediates cardiac myocyte apoptosis via endotoxin. Am J Physiol Heart Circ Physiol. 2002; 282(5):H1907–14. Epub 2002/04/18. doi: 10.1152/ajpheart.00393.2001 PMID: 11959658.

20. Claycomb WC, Lanson NA Jr., Stallworth BS, Egeland DB, Delcarpio JB, Bahinski A, et al. HL-1 cells: a cardiac muscle cell line that contracts and retains phenotypic characteristics of the adult cardiomyocyte. Proc Natl Acad Sci U S A. 1998; 95(6):2979–84. Epub 1998/04/18. PMID: 9501201; PubMed Central PMCID: PMC19680.

21. Kitta K, Day RM, Ikeda T, Suzuki YJ. Hepatocyte growth factor protects cardiac myocytes against oxidative stress-induced apoptosis. Free Radic Biol Med. 2001; 31(7):902–10. Epub 2001/10/05. S0891584901006633 [pii]. PMID: 11585709.

22. Yuan Z, McCauley R, Chen-Scarabelli C, Abounit K, Stephanou A, Barry SP, et al. Activation of Src protein tyrosine kinase plays an essential role in urocortin-mediated cardioprotection. Mol Cell Endocrinol. 2010; 325(1–2):1–7. Epub 2010/04/27. S0303-7207(10)00230-3 [pii] doi: 10.1016/j.mce.2010.04.013 PMID: 20416357.

23. Webster KA, Discher DJ, Kaiser S, Hernandez O, Sato B, Bishopric NH. Hypoxia-activated apoptosis of cardiac myocytes requires reoxygenation or a pH shift and is independent of p53. The Journal of clinical investigation. 1999; 104(3):239–52. doi: 10.1172/JCI5871 PMID: 10430605; PubMed Central PMCID: PMC408414.

24. White SM, Constantin PE, Claycomb WC. Cardiac physiology at the cellular level: use of cultured HL-1 cardiomyocytes for studies of cardiac muscle cell structure and function. Am J Physiol Heart Circ Physiol. 2004; 286(3):H823–9. Epub 2004/02/10. doi: 10.1152/ajpheart.00986.2003 286/3/H823 [pii]. PMID: 14766671.

25. Andersen AD, Poulsen KA, Lambert IH, Pedersen SF. HL-1 mouse cardiomyocyte injury and death after simulated ischemia and reperfusion: roles of pH, Ca2+-independent phospholipase A2, and Na +/H+ exchange. Am J Physiol Cell Physiol. 2009; 296(5):C1227–42. Epub 2009/03/06. 00370.2008 [pii] doi: 10.1152/ajpcell.00370.2008 PMID: 19261908.

26. Fiedler B, Feil R, Hofmann F, Willenbockel C, Drexler H, Smolenski A, et al. cGMP-dependent protein kinase type I inhibits TAB1-p38 mitogen-activated protein kinase apoptosis signaling in cardiac myocytes. J Biol Chem. 2006; 281(43):32831–40. Epub 2006/09/01. M603416200 [pii] doi: 10.1074/jbc.M603416200 PMID: 16943189.

27. Anderson ME, Meister A. Glutathione monoesters. Anal Biochem. 1989; 183(1):16–20. Epub 1989/11/15. 0003-2697(89)90164-4 [pii]. PMID: 2619041.

28. Du Y, Ko KM. Effects of emodin treatment on mitochondrial ATP generation capacity and antioxidant components as well as susceptibility to ischemia-reperfusion injury in rat hearts: single versus multiple doses and gender difference. Life Sci. 2005; 77(22):2770–82. Epub 2005/06/21. S0024-3205(05)00537-0 [pii] doi: 10.1016/j.lfs.2005.03.027 PMID: 15964600.

29. Dwivedi VK, Chandra M, Misra PC, Misra A, Misra MK. Status of some free radical scavenging enzymes in the blood of myocardial infarction patients. J Enzyme Inhib Med Chem. 2006; 21(1):43–6. Epub 2006/03/31. doi: 10.1080/14756360500286070 PMID: 16570504.

30. Rozanski GJ, Xu Z. Glutathione and K(+) channel remodeling in postinfarction rat heart. Am J Physiol Heart Circ Physiol. 2002; 282(6):H2346–55. Epub 2002/05/11. doi: 10.1152/ajpheart.00894.2001 PMID: 12003845.

31. Seefeldt T, Zhao Y, Chen W, Raza AS, Carlson L, Herman J, et al. Characterization of a novel dithiocarbamate glutathione reductase inhibitor and its use as a tool to modulate intracellular glutathione. J Biol Chem. 2009; 284(5):2729–37. Epub 2008/12/04. M802683200 [pii] doi: 10.1074/jbc.M802683200 PMID: 19049979; PubMed Central PMCID: PMC2631970.

32. Xie J, Potter A, Xie W, Lynch C, Seefeldt T. Evaluation of a dithiocarbamate derivative as a model of thiol oxidative stress in H9c2 rat cardiomyocytes. Free Radic Biol Med. 2014; 70:214–22. Epub 2014/03/13. doi: 10.1016/j.freeradbiomed.2014.02.022 PMID: 24607690; PubMed Central PMCID: PMC4011664.

33. Zhao Y, Seefeldt T, Chen W, Carlson L, Stoebner A, Hanson S, et al. Increase in thiol oxidative stress via glutathione reductase inhibition as a novel approach to enhance cancer sensitivity to X-ray irradiation. Free Radic Biol Med. 2009; 47(2):176–83. Epub 2009/04/29. S0891-5849(09)00237-8 [pii] doi: 10.1016/j.freeradbiomed.2009.04.022 PMID: 19397999; PubMed Central PMCID: PMC2745482.

34. Zhao Y, Seefeldt T, Chen W, Wang X, Matthees D, Hu Y, et al. Effects of glutathione reductase inhibition on cellular thiol redox state and related systems. Arch Biochem Biophys. 2009; 485(1):56–62. Epub 2009/03/11. S0003-9861(09)00064-2 [pii] doi: 10.1016/j.abb.2009.03.001 PMID: 19272349; PubMed Central PMCID: PMC2709784.

35. Logan SJ, Yin L, Geldenhuys WJ, Enrick MK, Stevanov KM, Carroll RT, et al. Novel thiazolidinedione mitoNEET ligand-1 acutely improves cardiac stem cell survival under oxidative stress. Basic Res Cardiol. 2015; 110(2):19. Epub 2015/03/03. doi: 10.1007/s00395-015-0471-z PMID: 25725808.

36. Frantz S, Bauersachs J, Ertl G. Post-infarct remodelling: contribution of wound healing and inflammation. Cardiovasc Res. 2009; 81(3):474–81. Epub 2008/11/04. cvn292 [pii] doi: 10.1093/cvr/cvn292 PMID: 18977766; PubMed Central PMCID: PMC2639128.

37. Grieve DJ, Shah AM. Oxidative stress in heart failure. More than just damage. Eur Heart J. 2003; 24 (24):2161–3. Epub 2003/12/09. S0195668X03006912 [pii]. PMID: 14659766.

38. Venardos KM, Perkins A, Headrick J, Kaye DM. Myocardial ischemia-reperfusion injury, antioxidant enzyme systems, and selenium: a review. Curr Med Chem. 2007; 14(14):1539–49. Epub 2007/06/23. PMID: 17584062.

39. Jiao XY, Gao E, Yuan Y, Wang Y, Lau WB, Koch W, et al. INO-4885 [5,10,15,20-tetra[N-(benzyl-4'-carboxylate)-2-pyridinium]-21H,23H-porphine iron(III) chloride], a peroxynitrite decomposition catalyst, protects the heart against reperfusion injury in mice. J Pharmacol Exp Ther. 2009; 328(3):777–84. Epub 2008/11/27. jpet.108.144352 [pii] doi: 10.1124/jpet.108.144352 PMID: 19033557; PubMed Central PMCID: PMC2663530.

40. Yang H, Gu L, Zhang L, Yan M, Zheng X. Involvement of hydrogen peroxide in the manganese-induced myocytes mitochondrial membrane potential loss. Toxicol Mech Methods. 2009; 19(1):66–72. Epub 2009/09/26. doi: 10.1080/15376510802428583 PMID: 19778235.

41. Fang YZ, Yang S, Wu G. Free radicals, antioxidants, and nutrition. Nutrition. 2002; 18(10):872–9. Epub 2002/10/04. S0899900702009164 [pii]. PMID: 12361782.

42. Wiley SE, Andreyev AY, Divakaruni AS, Karisch R, Perkins G, Wall EA, et al. Wolfram Syndrome protein, Miner1, regulates sulphydryl redox status, the unfolded protein response, and Ca2+ homeostasis. EMBO molecular medicine. 2013; 5(6):904–18. doi: 10.1002/emmm.201201429 PMID: 23703906; PubMed Central PMCID: PMC3779451.

43. Chang NC, Nguyen M, Germain M, Shore GC. Antagonism of Beclin 1-dependent autophagy by BCL-2 at the endoplasmic reticulum requires NAF-1. The EMBO journal. 2010; 29(3):606–18. doi: 10.1038/emboj.2009.369 PMID: 20010695; PubMed Central PMCID: PMC2830692.

44. Dhalla NS, Elmoselhi AB, Hata T, Makino N. Status of myocardial antioxidants in ischemia-reperfusion injury. Cardiovasc Res. 2000; 47(3):446–56. Epub 2000/08/30. S0008-6363(00)00078-X [pii]. PMID: 10963718.

45. Landry AP, Cheng Z, Ding H. Reduction of mitochondrial protein mitoNEET [2Fe-2S] clusters by human glutathione reductase. Free Radic Biol Med. 2015; 81:119–27. Epub 2015/02/04. doi: 10.1016/j.freeradbiomed.2015.01.017 PMID: 25645953; PubMed Central PMCID: PMC4365936.

46. Belka C. The fate of irradiated tumor cells. Oncogene. 2006; 25(7):969–71. Epub 2005/10/26. 1209175 [pii] doi: 10.1038/sj.onc.1209175 PMID: 16247448.

47. Sadhu SS, Callegari E, Zhao Y, Guan X, Seefeldt T. Evaluation of a dithiocarbamate derivative as an inhibitor of human glutaredoxin-1. J Enzyme Inhib Med Chem. 2012. Epub 2012/02/04. doi: 10.3109/14756366.2011.649267 PMID: 22299579.